Chapter

Nanostructured Transition Metal Compounds as Highly Efficient Electrocatalysts for Dye-Sensitized Solar Cells

Yi-June Huang and Chuan-Pei Lee

Abstract

Nowadays, the requirement of energy increases every year, however, the major energy resource is fossil fuel, a limiting source. Dye-sensitized solar cells (DSSCs) are a promising renewable energy source, which could be the major power supply for the future. Recently, the transition metal component has been demonstrated as potential material for counter electrode of platinum (Pt)-free DSSCs owing to their excellent electrocatalytic ability and their abundance on earth. Furthermore, the transition metal components exist different special nanostructures, which provide high surface area and various electron transport routs during electrocatalytic reaction. In this chapter, transition metal components with different nanostructures used for the application of electrocatalyst in DSSCs will be introduced; the performance of electrocatalyst between intrinsic heterogeneous rate constant and effective electrocatalytic surface area are also be clarified. Final, the advantages of the electrocatalyst with different dimensions (i.e., one to three dimension structures) used in DSSCs are also summarized in the conclusion.

Keywords: counter electrode, dye-sensitized solar cells, nanostructures, and transition metal components

1. Introduction

In this century, the energy requisition and environment caring arrive at the highest point in history. The clean and economical renewable energy resource is urgently needed for us. Photovoltaics, named solar cells, tremendous progress has been achieved in efficiency (η), reproducibility, and stability [1–3]. It has been considered as one of the most promising renewable energy sources. Photovoltaics are classified to three generations, as shown in **Figure 1** [1, 4–7]. The first-generation solar cells, named silicon-based solar cells or the traditional solar cells, made up of crystalline silicon. These solar cells demonstrate high efficiency and significant demand in the market, but the production cost of crystalline silicon materials limited the large-scale industrial applications. The second-generation is cadmium telluride (CdTe)/cadmium indium gallium diselenide (CIGS) based solar cells. The solar cells could be produced with large-scale and well efficiency (14–22%). The first and second generations are the most widely solar cells at present. However, they are scarcity, the toxicity of materials, high-temperature, and high-vacuum processes

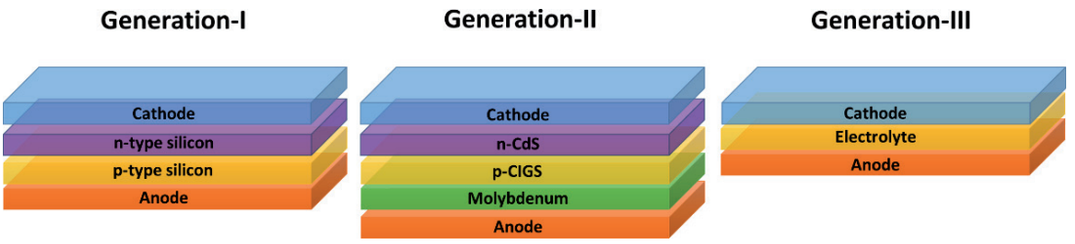

Figure 1.
The scheme of three generation photovoltaic solar cells.

that restrict further applications. Dye-sensitized solar cells (DSSCs), classed third-generation solar cells, have gained attention and be regarded as prospective solar cells for the photovoltaic technologies in recent years as potential cost-effective alternatives to the first and second generations solar cells [8–11]. Furthermore, the DSSCs have outstanding performance in an indoor, dim light environment [12–14].

Typically, DSSCs are consist of three sections, including photoanode, electrolyte, and counter electrode (CE), that respond to different functions, as shown in **Figure 2** [1, 4, 5, 8–10]. The photoanode converts the photon into the electron by the dye. The electrolyte keeps the function of the photoanode by iodine ion. The CE catalyzes the redox reduction in the electrolyte, which is an obvious influence on the photovoltaic performance, long-term stability, and cost of the device. In other words, the CE is a crucial component of DSSCs.

The CE is classified into three components, that are electrocatalyst, transparent conducting oxide, and substrate, as shown in **Figure 2**. Among them, the electrocatalyst is the key factor to promise the function of CE [1, 7–9, 15, 16]. As shown in **Figure 3**, between electrolyte and CE, the reaction of reduction iodide/triiodide (I^-/I_3^-) redox couple is that: The first stage, diffusion, triiodide diffuses from electrolyte bulk to near the CE for regenerating electrolyte. The second stage, decomposition, triiodide decomposes to iodide and iodine. The iodide is used to renew the dye and iodine will go to the next step. The third stage, adsorption, the CE adsorbs iodine near the CE. The fourth stage, electrocatalysis, electrocatalyst catalyzes reduction reaction, transferring iodine to iodide. The final stage, desorption, the CE desorbs iodide to complete regenerate the electrolyte. According to this mechanism, the electrocatalytic ability, it also represents the reaction rate in here, and the specific structure are the major affections for the reduction reaction.

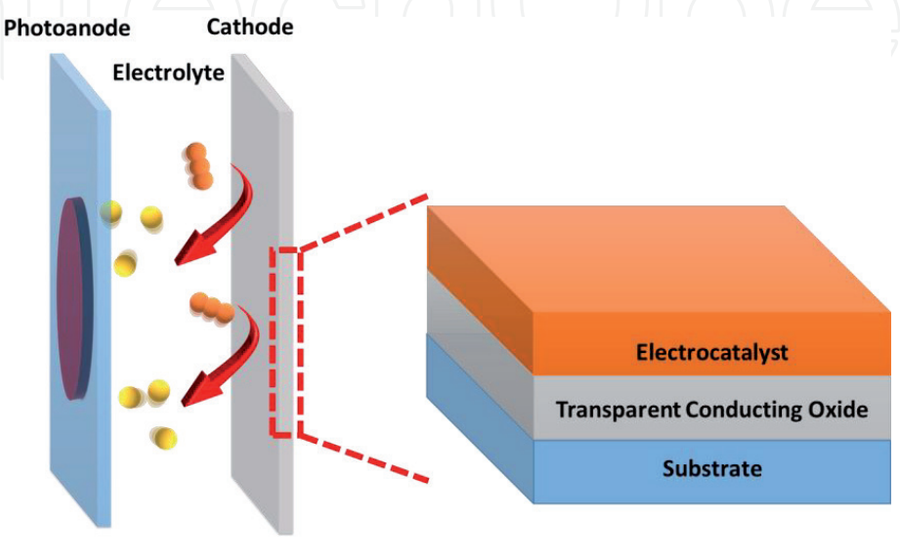

Figure 2.
The scheme of dye-sensitized solar cells and counter electrode (cathode).

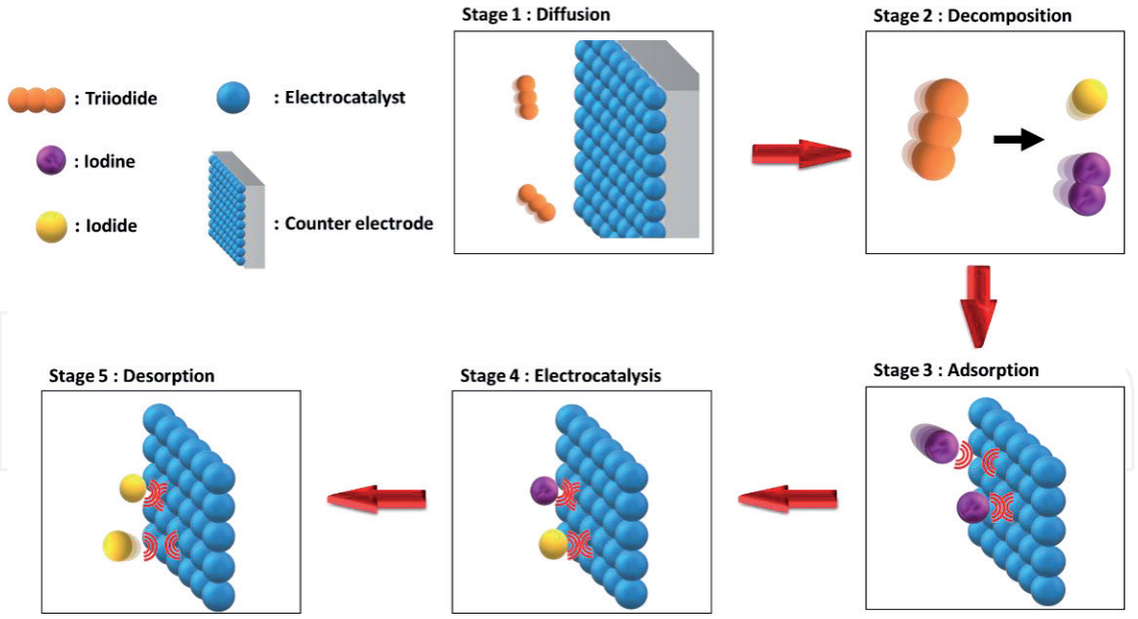

Figure 3.
The scheme of reduction iodide/triiodide (I^-/I_3^-) redox couple in counter electrode.

The traditional electrocatalyst of DSSCs is Platinum (Pt), which has an outstanding electrocatalytic ability [10, 15–20]. However, Pt, noble metal, is rare on earth that present expensive prices and difficult shapes the specific structure. Up to date, there are a few non-Pt nanomaterials that could have comparable electrocatalytic ability to that of Pt. There have two ways to raise the electrocatalytic reduction reaction. The intrinsic electrocatalytic ability of the electrocatalyst is directly related the electrocatalytic ability. In other words, the choice of material is very important. The other way is to design the nanostructure of the electrocatalyst for I_3^- reduction regarding with the charge transfer route and the surface area.

Transition metal compounds (TMCs) possess d-electron filling in e_g orbitals, which promote excellent electrocatalytic performance in partially filled condition [4, 19, 21–24]. So, they are interested to replace Pt. But most of TMCs still show poorer electrocatalytic ability than Pt. To overcome the challenge, TMCs are synthesized with various nanostructure, which is an important factor for increasing electrocatalytic ability [20–22, 25]. A nanostructure is defined if any dimension of the structure is lower than 100 nm, the structure is the nanostructure. Basically, nanostructure divides into four groups: zero-dimensional (0D, *e.g.* nanoparticle, nanocube, *etc.*), one-dimensional (1D, *e.g.* nanorod, nanotube, nanoneedle, *etc.*), two-dimensional (2D, *e.g.* nanosheet, nanopental *etc.*) and hierarchical nanostructures, as shown in **Figure 4**. In view of 1D, 2D, and hierarchical nanostructures have

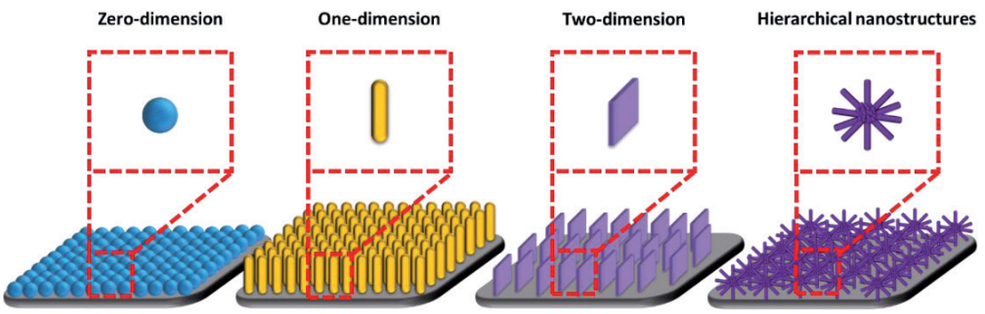

Figure 4.
The scheme of zero-dimensional (0D), one-dimensional (1D), two-dimensional (2D), and hierarchical nanostructure.

complex structure. In this chapter, we will systematically discuss their plural strategies (including high electrochemical surface area, directional electron transferring pathways, decrease diffusion control, *etc.*) to promote the electrocatalytic ability for DSSCs performance.

2. One-dimensional nanostructure (1D)

One-dimensional TMCs nanostructure is expected that it provides the 1D electron transfer pathways, promoting electrolyte penetration, and more reaction area [26–34]. However, the vertical 1D structure is rarely obtained because it is difficult to synthesize. Herein, we focus on that the 1D structure has been directly obtained without the template method, in **Figures 5** and **6**. Their corresponding efficiencies are listed in **Table 1**. In **Figure 5**, it shows horizontal 1D TMCs nanostructure SEM images of MoN nanorod, $W_{18}O_{49}$ nanowire, NiS nanorod, $CoSe_2$ nanorod, $Co_{0.85}Se$ nanotubes, $CoSe_2/CoSeO_3$ nanorod, and Ni_3S_4 nanorod that were synthesized by Song et al., Zhou et al., Yang et al., Sun et al., Yuan et al., Huang et al., and Huang et al., respectively [27–33]. Song et al. reported that MoN nanorod morphology reveals enhancement of diffusion kinetics for the active electrochemical process, as shown in **Figure 5a** [27]. So that the MoN nanorod has higher V_{OC} and J_{SC} than MoN nanoparticle. Zhou synthesized $W_{18}O_{49}$ nanowire (**Figure 5b**), having oxygen vacancies within the range of $WO_{2.625}$ to WO_3, *via* the solvothermal method [28]. Their efficiency is 4.85% for Co ion electrolyte. Yang et al. obtained NiS nanorod (**Figure 5c**), which is α type, through chemical bath method [29]. It has η of 5.20%,

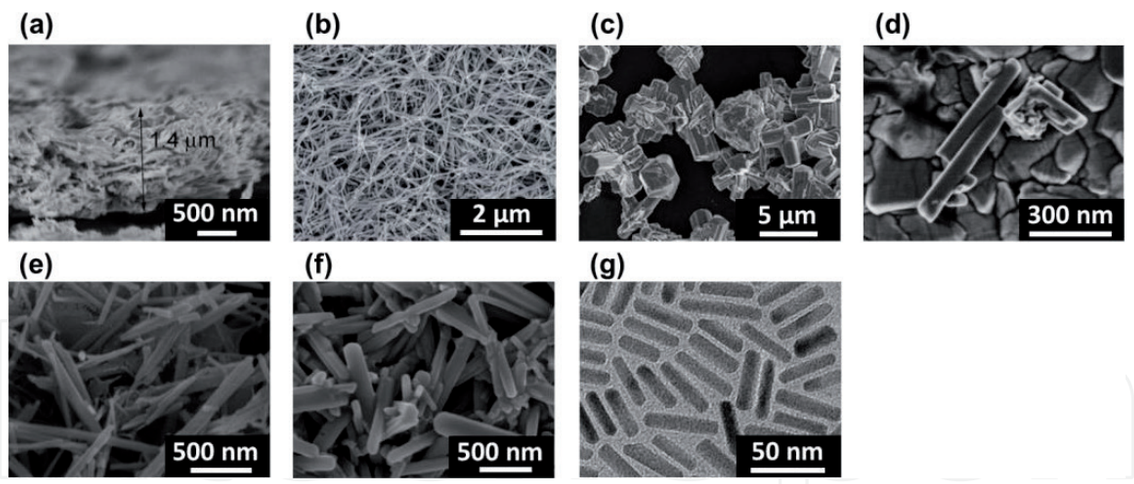

Figure 5.
The SEM of horizontal 1D nanostructure with (a) MoN, (b) $W_{18}O_{49}$, (c) NiS, (d) $CoSe_2$, (e) $Co_{0.85}Se$, (f) $CoSe_2/CoSeO_3$, (g) Ni_3S_4 [27–33].

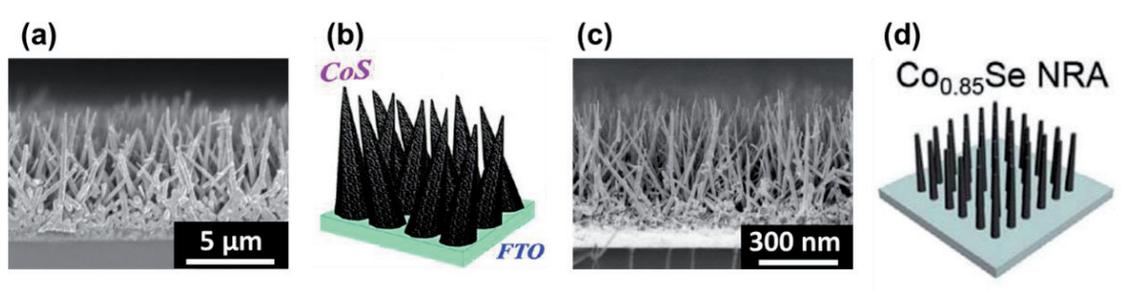

Figure 6.
The pseudo-vertical 1D nanostructure with (a) and (b) CoS and (c) and (d) $Co_{0.85}Se$ [26, 34].

Materials	η (%)	V_{OC} (V)	J_{SC} (mA cm^{-2})	FF	η/η_{Pt}	Ref
CoS	7.67	0.71	16.31	0.66	1.00	[26]
MoN	7.29	0.74	15.26	0.65	0.98	[27]
$W_{18}O_{49}$	4.85	0.80	9.26	0.67	1.08	[28]
NiS	5.20	0.68	11.42	0.67	0.83	[29]
$CoSe_2$	10.20	0.75	18.55	0.73	1.25	[30]
$Co_{0.85}Se$	5.34	0.71	14.51	0.52	0.71	[31]
$CoSe_2/CoSeO_3$	7.54	0.82	14.32	0.64	0.95	[32]
Ni_3S_4	7.31	0.75	15.53	0.63	0.93	[33]
$Co_{0.85}Se$	8.35	0.74	15.76	0.71	1.08	[34]

Table 1.
A partial list of literature on the DSSCs with 1D TMCs nanostructure based CEs.

which is better than the nanoparticle NiS (4.20%). The reason is that the nanorod affords lower charge transfer resistance than the nanoparticle. Sun et al. acquired $CoSe_2$ nanorod (**Figure 5d**), possessing a single orthorhombic crystal structure, by hydrothermal method [30]. The $CoSe_2$ nanorod exits the excellent performance (10.20%), even better than the Pt. They remind that single $CoSe_2$ nanorod has great electrocatalytic ability, lower charge resistance, and higher adsorption capacity for electrolyte. Yuan et al. prepared $Co_{0.85}Se$ nanotubes (**Figure 5e**) by a simple hydrothermal method [31]. It shows η of 5.34%, which lower than Pt, obviously. Huang et al. obtained $CoSe_2/CoSeO_3$ nanorod (**Figure 5f**) through a microemulsion-assisted hydrothermal synthesis [32]. It reveals η of 7.54%, which is approach Pt performance. This result contributes to the 1D electron transfer pathways. Huang et al. synthesized the Ni_3S_4 nanorod (**Figure 5g**) *via* a one-pot colloidal synthesis [33]. And it has η of 7.31%, which is quite close Pt. As listed in **Table 1**, there have a few of the 1D TMCs nanostructures existing the better performance than the Pt.

Most of them are vertical 1D TMCs nanostructures. The horizontal 1D TMCs nanostructures could not support the vertical electron transfer pathways and promote the electrolyte penetration. So most of them display lower performance than the Pt.

The vertical 1D TMCs nanostructure is an ideal condition, as shown in **Figure 4**. Kung et al. and Jin et al. directly synthesized pseudo-vertical 1D nanostructure array with CoS and $Co_{0.85}Se$, respectively, as shown in **Figure 6** [26, 34]. This structure sufficiently acts the 1D TMCs nanostructure advantages, including favorable for fast diffusion of redox species within the CE film, 1D direction electron channel, enhance electrolyte penetration, and more reaction area. Both of them exhibit higher value of η than Pt. In other words, they could straightly replace the Pt function for CE in DSSCs.

3. Two-dimensional (2D)

Geim and Grigorieva classified 2D materials into three groups [35]. First group, graphene type contains graphene, fluorographene, graphene oxide, hBN, *etc.*; second group, 2D chalcogenides (transition metal) type includes MoS_2, NbS_2, $NbSe_2$, $CoSe_2$, $MoSe_2$, $ZrSe_2$, GaSe, GaTe, InSe, Bi_2Se_3, Bi_2Te_3, *etc.*; final group, 2D oxides type involves TiO_2, MnO_2, V_2O_5, RuO_2, perovskite-based materials ($LaNb_2O_7$, $Ba_4Ti_3O_{12}$, $Ca_2Ta_2TiO_{10}$ *etc.*), hydroxides ($Ni(OH)_2$, $Eu(OH)_2$, *etc.*), *etc*. Research of 2D TMCs

nanostructure is intensified in recently [16, 36]. The bandgap energy is reduced by decreasing the layer of the TMCs [16, 35, 37–40]. In other words, a single or a few layers of the 2D TMCs nanostructure presents excellent electrocatalytic ability. Besides that, the 2D TMCs nanostructure has advantages including enhancing the diffusion of electrolyte, vertical electron channel, and special optical property.

In this section, the partial works of literature are chosen depending on the electrocatalytic performance and structure. Their corresponding SEM images and efficiency parameters are shown in **Figures 7** and **8**, and **Table 2**, respectively. In **Figure 7**, Ibrahem et al., Huang et al., and Mohammadnezhad et al. applied the horizontal 2D nanostructure with $NbSe_2$, $MoSe_2$, and $Cu_2ZnSnS_xSe_{4-x}$ in CE for DSSCs [41–43]. Ibrahem et al. reported that the $NbSe_2$ nanosheet (**Figure 7a**) has the best performance among nanosheet, nanorod, and nanoparticle [41]. They mention that nanosheet could provide high surface area and coverage. And the $NbSe_2$ nanosheet existed η of 7.73%, which is better than the Pt CE. The result indicates that $NbSe_2$ nanosheet substitutes to the noble metal Pt in DSSCs. Following the idea, $MoSe_2$ and $Cu_2ZnSnS_xSe_{4-x}$ nanosheet show the η of 7.58% and 5.73%, respectively. However, both of their values of η are lower than the Pt. To increase the performance of 2D TMCs nanostructure, the pseudo-vertical 2D nanostructure was synthesized and provide the vertical electron channel. The pseudo-vertical 2D nanostructure with MoS_2, $CoSe_2$, MoS_2, $Cu_xZn_ySn_zS$, and $CoNi_2S_4$ were obtained by Antonelou et al., Chiu et al., Raj et al., Chiu et al., and Patil et al., respectively [44–48]. Antonelou et al. obtained the MoS2 nanosheet with η of 8.40%, which has thicknesses down to the 1-2 nm scale. Chiu et al. acquired the nanoclimbing-wall-like $CoSe_2$ (**Figure 8a**) through an electrodeposition process, by using bathes with different pH values.

Its performance is 8.92%. They mentioned that vertical nanowall provides conducting charge for electrocatalytic reduction, as shown in **Figure 9a**. Raj et al. synthesized reflectivity of MoS_2 nanosheet (**Figure 8b**), which has η of 7.50%, through chemical vapor deposition (CVD). The reflectivity of MoS_2 nanosheet is

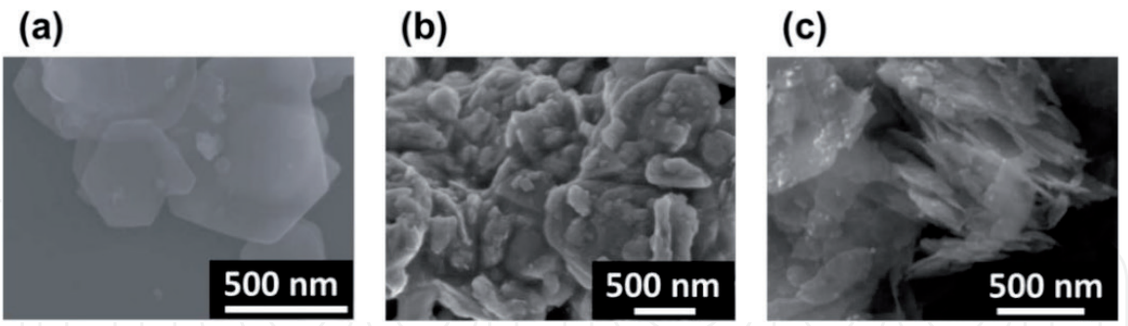

Figure 7.
The SEM of 2D nanostructure with (a) $NbSe_2$, (b) $MoSe_2$, (c) $Cu_2ZnSnS_xSe_{4-x}$ [41–43].

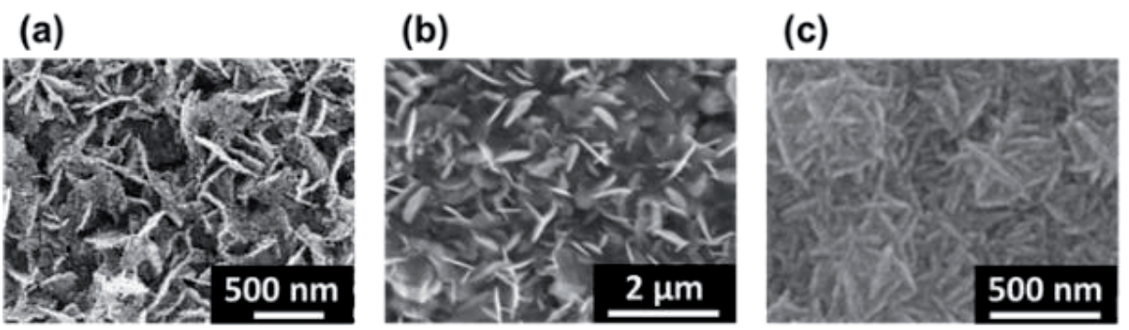

Figure 8.
The pseudo-vertical 2D nanostructure with (a) $CoSe_2$, (b) MoS_2, and (c) $CoNi_2S_4$ [45–48].

Materials	η (%)	V_{OC} (V)	J_{SC} (mA cm^{-2})	FF	η/η_{Pt}	Ref
$NbSe_2$	7.73	0.74	16.85	0.62	1.10	[41]
MoS_2	8.40	0.74	22.60	0.50	0.97	[44]
$CoSe_2$	8.92	0.73	18.03	0.67	1.08	[45]
$MoSe_2$	7.58	0.70	15.97	0.67	0.97	[42]
MoS_2	7.50	0.71	15.20	0.70	1.03	[46]
$Cu_xZn_ySn_zS$	7.44	0.67	16.57	0.66	1.03	[47]
$CoNi_2S_4$	8.86	0.66	19.21	0.70	0.98	[48]
$Cu_2ZnSnS_xSe_{4-x}$	5.73	0.69	12.60	0.66	0.99	[43]

Table 2.
A partial list of literature on the DSSCs with 2D TMCs nanostructure based CEs.

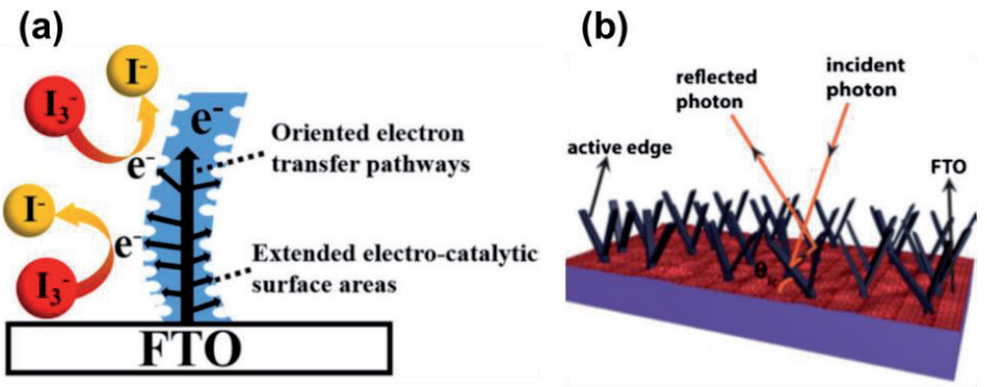

Figure 9.
The mechanism of 2D nanostructure with (a) $CoSe_2$ and (b) MoS_2 [45, 46].

raised their high reflectivity facilitates the absorbance of more photons, and more active edge sites exposed to redox couple in the electrolyte, as shown in **Figure 9b**. Chiu et al. gained $Cu_xZn_ySn_zS$ nanowall-structure by thermal solvent method, and it shows performance 7.44%. The performance is attributed to improves the carrier transport pathway and effectively reduces the interface resistance. Patil et al. utilized a simple one-step solution-based fabrication method for $CoNi_2S_4$ interconnected nanosheet (**Figure 8c**). The $CoNi_2S_4$ exhibits η of 8.86%, which attributes to a larger active surface area with favorable charge transport. The pseudo-vertical 2D nanostructure has obviously improvement of electrocatalytic ability than the normal 2D nanostructure. It is not only providing vertical transport pathways and active surface area but also contributes to reflection photon. Those properties make 2D TMCs nanostructure have the potential to alternative Pt as an electrocatalyst.

4. Hierarchical nanostructure

Basically, 0D nanostructure possesses a high reaction area; 1D and 2D nanostructure offers directional electron pathways and enhance electrolyte penetration. But they have their own weakness. For example, 0D nanostructure is easy aggregation and has larger heterogeneous resistance; 1D and 2D nanostructure have lower reaction area. A hierarchical nanostructure consists of the nanostructure with multidimensional subunits (0D, 1D, and 2D). It merges various subunits, so it has

multidimensional nanostructure advantages, including high reaction area, benefit electron transfer, avoiding aggregation, enhance electrolyte diffusion, and offer directional electron pathways.

Herein, we list partial literature with hierarchical TMCs nanostructure. **Figure 10** shows SEM of Ni_3Se_4 with sea urchins-like structure, $TiO_{1.1}Se_{0.9}$ with nanospheres and 1D nanorods, $NiCo_{0.2}$ with hollow structure and nanoclusters, $NiCo_2S_4$ with ball-in-ball structure, $NiS@MoS_2$ with feather duster-like hierarchical structure, $CoSe_2/CoSeO_3$ with hierarchical urchin-like structure, CuO/Co_3O_4 with core-shell structure and $CoS_2/NC@Co\text{-}WS_2$ with yolk-shell structure by Lee et al., Li et al., Jiang et al., Jiang et al., Su et al., Huang et al., Liao et al., and Huang et al., respectively [49–56]. And their efficiency parameters are listed in **Table 3**. Lee et al. synthesized the Ni_3Se_4 sea urchins-like structure (**Figure 10a**) through one-step and low temperature hydrothermal process [49]. It reveals η of 8.31%, which attribute to the high active electrocatalytic surface area. Li et al. obtained $TiO_{1.1}Se_{0.9}$ with nanospheres and 1D nanorods (**Figure 10b**) *via* a simple dip-coating process and rapid thermal annealing (RTA) process [50]. The $TiO_{1.1}Se_{0.9}$ exhibits η of 9.47%, which is better than the Pt. The result is established that the nanospheres can work as electro-catalytic active sites, and the nanorods can function not only as electro-catalytic active sites but also as fast electron transport channels, as shown in **Figure 11a**. Jiang et al. synthesized $NiCo_{0.2}$ hollow structure and nanoclusters, having uniform spherical particles with an average diameter of about 2 μm and shell thickness of around 200 nm (**Figure 10c**), *via* a thermal method [51]. It shows η of 9.30% and displays that the novel spherical structures can efficiently promote the transfer of electrons from the conductive carbon frameworks to metal nanoparticles, thus resulting in high electrocatalytic activity for the reduction. Jiang et al. acquired $NiCo_2S_4$ ball-in-ball structure (**Figure 10d**) by a thermal method [52]. Its efficiency is 9.49%, which is attributed to the rougher surface, higher surface area, and high diffusion coefficient for redox. Su et al. obtained $NiS@MoS_2$ feather duster-like hierarchical structure, which has η of 8.58% [53]. They propose that feather duster-like hierarchical structure array can support the fast electron transfer and electrolyte diffusion channels, moreover, it also can render abundant active catalytic sites and large electron injection efficiency from CE to the electrolyte. Huang et al. gained $CoSe_2/CoSeO_3$ hierarchical urchin-like structure (**Figure 10g**), the nanoparticle-composed sphere is the central core with a diameter of about 50 nm surrounded by several hexagonal prisms, through a one-step hydrothermal method [54]. The $CoSe_2/CoSeO_3$ reveals η of 9.29% and is mention that the

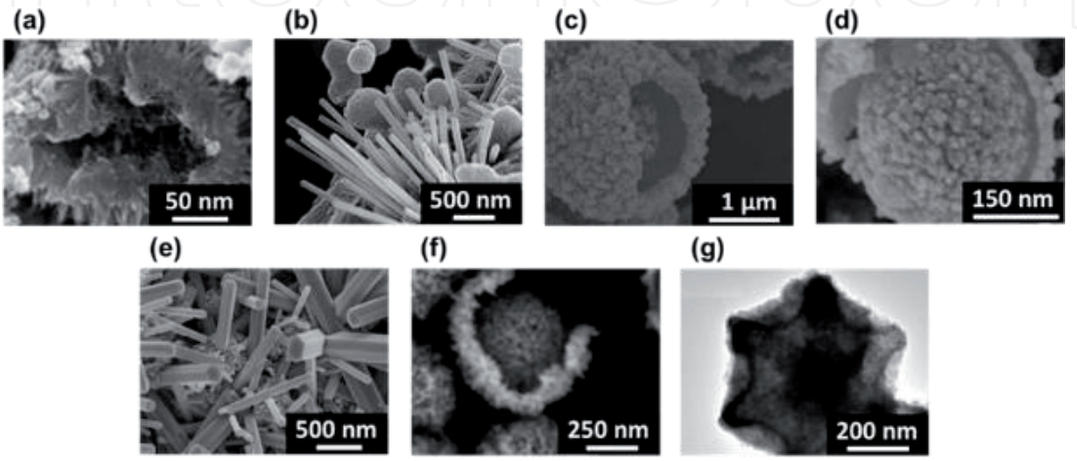

Figure 10.
The SEM of hierarchical nanostructure with (a) Ni_3Se_4, (b) $TiO_{1.1}Se_{0.9}$, (c) $NiCo_{0.2}$, (d) $NiCo_2S_4$, (e) $CoSe_2/CoSeO_3$, (f) CuO/Co_3O_4, and (g) $CoS_2/NC@Co\text{-}WS_2$ [49–56].

Materials	η (%)	V_{OC} (V)	J_{SC} (mA cm^{-2})	FF	η/η_{Pt}	Ref
Ni_3Se_4	8.31	0.75	16.27	0.69	1.03	[49]
$TiO_{1.1}Se_{0.9}$	9.47	0.79	17.22	0.70	1.22	[50]
$NiCo_{0.2}$	9.30	0.78	17.80	0.67	1.16	[51]
$NiCo_2S_4$	9.49	0.84	17.40	0.647	1.14	[52]
$NiS@MoS_2$	8.58	0.77	16.64	0.67	1.05	[53]
$CoSe_2/CoSeO_3$	9.29	0.82	16.09	0.70	1.12	[54]
CuO/Co_3O_4	8.34	0.73	18.13	0.63	1.06	[55]
CoS_2/NC@Co-WS_2	9.21	0.82	16.50	0.67	1.13	[56]

Table 3.
A partial list of literature on the DSSCs with hierarchical TMCs nanostructure based CEs.

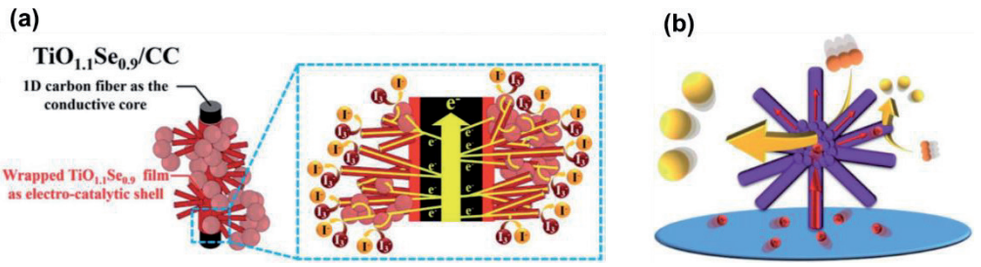

Figure 11.
The mechanism of hierarchical nanostructure with (a) $TiO_{1.1}Se_{0.9}$ and (b) $CoSe_2/CoSeO_3$ [50, 54].

urchin-like structure possessing the hexagonal prism structure and nanoparticles to provide both rapid electron transport routes and a reasonably high surface area for electro-catalytic reactions, as shown in **Figure 11b**. Liao et al. obtained CuO/Co_3O_4 core-shell structure (**Figure 10f**) *via* a facile self-templated method [55]. The CuO/Co_3O_4 has η of 8.34% and an excellent electronic transmission channel and more adsorption sites for the redox couple, which greatly enhances the subsequent redox process. Huang et al. acquired CoS_2/NC@Co-WS_2 with yolk-shell structure (**Figure 10g**) [56]. By virtue of larger surface area and more effective active sites, the CoS_2/NC@Co-WS_2 (η of 9.21%) has better performance than the Pt.

In this section, it can be found that the hierarchical TMCs nanostructure has better performance than the Pt in CE. In other words, they can efficiently raise the TMCs performance, so the hierarchical TMCs nanostructure could replace Pt directly.

5. Conclusion

The electrocatalytic ability of catalysts is usually determined by below two points: one is the intrinsic electrocatalytic activity, and another is the nanostructure. The nanostructure of TMCs can briefly be classified into 0D, 1D, 2D, and hierarchical nanostructures; those have different properties and could obviously affect the electrocatalytic ability. Herein, the partial reports about DSSCs with the electrocatalysts having 1D, 2D, or hierarchical nanostructures are selected for introduction and discussion. 1D nanostructure possesses several advantages, including the 1D electron transfer pathways, promoting electrolyte penetration, avoiding stack problem, and high reaction area. However, not all the electrocatalysts with 1D nanostructure show better performance than the Pt in DSSC application. Some of them lied down

on substrate; so, the advantage on vertical electron transport rout is not given. Furthermore, as the stacking problem comes out, it will lose surface are for reaction. 2D nanostructures possess the active site on edges or defects, and their 2D structure could provide the benefits below, such as directional electron and diffusion channels; these properties boost their DSSC performances obviously. However, the stacking problem and poor activity on basal plane of 2D materials also retarding their practical performance in DSSCs. Hierarchical nanostructure incorporates the profits of subunits, so it displays high reaction area, benefit electron transport rout, avoiding aggregation, enhanced electrolyte diffusion, *etc*. Several reports already demonstrated that the TMCs with hierarchical nanostructures show excellent electrocatalytic ability in DSSCs; they even exhibit better electrocatalytic performance than that of Pt.

Acknowledgements

This work was supported by the Ministry of Science and Technology (MOST) of Taiwan, under grant numbers 107-2113-M-845-001-MY3.

Author details

Yi-June Huang[1] and Chuan-Pei Lee[2*]

1 Department of Chemical Engineering, National Taiwan University, Taiwan

2 Department of Applied Physics and Chemistry, University of Taipei, Taiwan

*Address all correspondence to: cplee@utaipei.edu.tw

References

[1] Mrinalini Madoori, Islavath Nanaji, Prasanthkumar Seelam, Giribabu Lingamallu, Stipulating low production cost solar cells all set to retail...! Chem Rec. 2019; 19; 661-674, DOI: 10.1002/tcr.201800106.

[2] Zhou Liang, Zhuang Zechao, Zhao Huihui, Lin Mengting, Zhao Dongyuan, Mai Liqiang, Intricate hollow structures: controlled synthesis and applications in energy storage and conversion. Advanced Materials. 2017; 29; 1602914-1602942, DOI: 10.1002/adma.201602914.

[3] Park Nam-Gyu, Segawa Hiroshi, Research direction toward theoretical efficiency in perovskite solar cells. ACS Photonics. 2018; 5; 2970-2977, DOI: 10.1021/acsphotonics.8b00124.

[4] Guo J., Liang S., Shi Y., Hao C., Wang X., Ma T., Transition metal selenides as efficient counter-electrode materials for dye-sensitized solar cells. Physical Chemistry Chemical Physics. 2015; 17; 28985-28992, DOI: 10.1039/c5cp04862a.

[5] Yun Sining, Qin Yong, Uhl Alexander R., Vlachopoulos Nick, Yin Min, Li Dongdong, Han Xiaogang, Hagfeldt Anders, New-generation integrated devices based on dye-sensitized and perovskite solar cells. Energy & Environmental Science. 2018; 121; 476-526, DOI: 10.1039/c7ee03165c.

[6] Hisham A. Maddah Vikas Berry, Sanjay K. Behura, Biomolecular photosensitizers for dye-sensitized solar cells: Recent developments and critical insights. Renewable and Sustainable Energy Reviews. 2020; 121; 109678-109702, DOI: 10.1016/j.rser.2019.109678.

[7] Kouhnavard Mojgan, Ludin Norasikin Ahmad, Ghaffari Babak V, Sopian Kamarozzaman, Ikeda Shoichiro, Carbonaceous materials and their advances as a counter electrode in dye-sensitized solar cells: challenges and prospects. ChemSusChem. 2015; 8; 1510-1533, DOI: 10.1002/cssc.201500004.

[8] Yun Sining, Hagfeldt Anders, Ma Tingli, Pt-free counter electrode for dye-sensitized solar cells with high efficiency. Advanced Materials. 2014; 26; 6210-6237, DOI: 10.1002/adma.201402056.

[9] Wu Jihuai, Lan Zhang, Lin Jianming, Huang Miaoliang, Huang Yunfang, Fan Leqing, Luo Genggeng, Lin Yu, Xie Yimin, Wei Yuelin, Counter electrodes in dye-sensitized solar cells. Chemical Society Reviews. 2017; 46; 5975-6023, DOI: 10.1039/c6cs00752j.

[10] Fakharuddin Azhar, Jose Rajan, Brown Thomas M., Fabregat-Santiago Francisco, Bisquert Juan, A perspective on the production of dye-sensitized solar modules. Energy & Environmental Science. 2014; 7; 3952-3981, DOI: 10.1039/c4ee01724b.

[11] Yuan Huihui, Wang Wei, Xu Di, Xu Quan, Xie Junjie, Chen Xinyu, Zhang Tao, Xiong Changjun, He Yunlong, Zhang Yumei, Liu Yan, Shen Hujiang, Outdoor testing and ageing of dye-sensitized solar cells for building integrated photovoltaics. Solar Energy. 2018; 165; 233-239, DOI: 10.1016/j.solener.2018.03.017.

[12] Cao Yiming, Liu Yuhang, Zakeeruddin Shaik Mohammed, Hagfeldt Anders, Grätzel Michael, Direct contact of selective charge extraction layers enables high-efficiency molecular photovoltaics. Joule. 2018; 2; 1108-1117, DOI: 10.1016/j.joule.2018.03.017.

[13] Cheng Rui, Chung Chih-Chun, Zhang Hong, Liu Fangzhou, Wang Wei-Ting, Zhou Zhiwen, Wang Sijia,

Djurišić Aleksandra B., Feng Shien-Ping, Tailoring triple-anion perovskite material for indoor light harvesting with restrained halide segregation and record high efficiency beyond 36%. Advanced Energy Materials. 2019; 1901980-1901987, DOI: 10.1002/aenm.201901980.

[14] Chen Han-Ting, Huang Yi-June, Li Chun-Ting, Lee Chuan-Pei, Lin Jiann T., Ho Kuo-Chuan, Boron nitride/sulfonated polythiophene composite electrocatalyst as the TCO and pt-free counter electrode for dye-sensitized solar cells: 21% at dim light. ACS Sustainable Chemistry & Engineering. 2020 8 5251-5259, DOI: 10.1021/acssuschemeng.0c00097.

[15] Wu Mingxing, Lin Xiao, Wang Yudi, Wang Liang, Guo Wei, Qi Daidi, Peng Xiaojun, Hagfeldt Anders, Gratzel Michael, Ma Tingli, Economical Pt-free catalysts for counter electrodes of dye-sensitized solar cells. Journal of the American Chemical Society. 2012; 134; 3419-3428, DOI: 10.1021/ja209657v.

[16] Singh Eric, Kim Ki Seok, Yeom Geun Young, Nalwa Hari Singh, Two-dimensional transition metal dichalcogenide-based counter electrodes for dye-sensitized solar cells. RSC Advances. 2017; 7; 28234-28290, DOI: 10.1039/c7ra03599c.

[17] Gao Min-Rui, Jiang Jun, Yu Shu-Hong, Solution-based synthesis and design of late transition metal chalcogenide materials for oxygen reduction reaction (ORR). Small. 2012; 8; 13-27, DOI: 10.1002/smll.201101573.

[18] Chen Wei-Fu, Iyer Shilpa, Iyer Shweta, Sasaki Kotaro, Wang Chiu-Hui, Zhu Yimei, Muckerman James T., Fujita Etsuko, Biomass-derived electrocatalytic composites for hydrogen evolution. Energy & Environmental Science. 2013; 6; 1818-1826, DOI: 10.1039/c3ee40596f.

[19] Kong Desheng, Cha Judy J., Wang Haotian, Lee Hye Ryoung, Cui Yi, First-row transition metal dichalcogenide catalysts for hydrogen evolution reaction. Energy & Environmental Science. 2013; 6; 3553-3558, DOI: 10.1039/c3ee42413h.

[20] Prasad Saradh, Durai G., Devaraj D., AlSalhi Mohamad Saleh, Theerthagiri J., Arunachalam Prabhakarn, Gurulakshmi M., Raghavender M., Kuppusami P., 3D nanorhombus nickel nitride as stable and cost-effective counter electrodes for dye-sensitized solar cells and supercapacitor applications. RSC Advances. 2018; 8; 8828-8835, DOI: 10.1039/c8ra00347e.

[21] Cui Xiaodan, Xie Zhiqiang, Wang Ying, Novel CoS_2 embedded carbon nanocages by direct sulfurizing metal-organic frameworks for dye-sensitized solar cells. Nanoscale. 2016; 8; 11984-11992, DOI: 10.1039/c6nr03052a.

[22] Li Chun-Ting, Tsai Yu-Lin, Ho Kuo-Chuan, Earth abundant silicon composites as the electrocatalytic counter electrodes for dye-sensitized solar cells. ACS Applied Materials & Interfaces. 2016; 8; 7037-7046, DOI: 10.1021/acsami.5b12423.

[23] Jiang Yiqing, Qian Xing, Niu Yudi, Shao Li, Zhu Changli, Hou Linxi, Cobalt iron selenide/sulfide porous nanocubes as high-performance electrocatalysts for efficient dye-sensitized solar cells. Journal of Power Sources. 2017; 369; 35-41, DOI: 10.1016/j.jpowsour.2017.09.080.

[24] Jian Siou-Ling, Huang Yi-June, Yeh Min-Hsin, Ho Kuo-Chuan, A zeolitic imidazolate framework-derived ZnSe/N-doped carbon cube hybrid electrocatalyst as the counter electrode for dye-sensitized solar cells. Journal of Materials Chemistry A. 2018; 6; 5107-5118, DOI: 10.1039/c8ta00968f.

[25] Li Chun-Ting, Chang Hung-Yu, Li Yu-Yan, Huang Yi-June, Tsai Yu-Lin, Vittal R., Sheng Yu-Jane, Ho Kuo-Chuan, Electrocatalytic zinc composites as the efficient counter electrodes of dye-sensitized solar cells: Study on the electrochemical performances and density functional theory calculations. ACS Applied Materials & Interfaces. 2015; 7; 28254-28263, DOI: 10.1021/acsami.5b07724.

[26] Kung Chung-Wei, Chen Hsin-Wei, Lin Chia-Yu, Huang Kuan-Chieh, Vitta R., Ho Kuo-Chuan, CoS acicular nanorod arrays for the counter electrode of an efficient dye-sensitized solar cell. ACS NANO. 2012; 6; 7016-7025, DOI: 10.1021/nn302063s.

[27] Song J., Li G. R., Xi Kai, Lei B., Gao X. P., Kumar R. Vasant, Enhancement of diffusion kinetics in porous MoN nanorods-based counter electrode in a dye-sensitized solar cell. Journal of Materials Chemistry A. 2014; 2; 10041-10047, DOI: 10.1039/c4ta01342e.

[28] Zhou Huawei, Shi Yantao, Dong Qingshun, Wang Liang, Zhang Hong, Ma Tingli, High electrocatalytic activity of $W_{18}O_{49}$ nanowires for cobalt complex and ferrocenium redox mediators. RSC Advances. 2014; 4; 42190-42196, DOI: 10.1039/c4ra07906j.

[29] Yang Xiao, Zhou Lei, Feng Ali, Tang Huaibao, Zhang Haijun, Ding Zongling, Ma Yongqing, Wu Mingzai, Jin Shaowei, Li Guang, Synthesis of nickel sulfides of different phases for counter electrodes in dye-sensitized solar cells by a solvothermal method with different solvents. Journal of Materials Research. 2014; 29; 935-941, DOI: 10.1557/jmr.2014.74.

[30] Sun Hong, Zhang Lu, Wang Zhong-Sheng, Single-crystal $CoSe_2$ nanorods as an efficient electrocatalyst for dye-sensitized solar cells. Journal of Materials Chemistry A. 2014; 2; 16023-16029, DOI: 10.1039/c4ta02238f.

[31] Yuan Hong, Jiao Qingze, Liu Jia, Liu Xiufeng, Li Yongjian, Shi Daxin, Wu Qin, Zhao Yun, Li Hansheng, Facile synthesis of $Co_{0.85}Se$ nanotubes/reduced graphene oxide nanocomposite as Pt-free counter electrode with enhanced electrocatalytic performance in dye-sensitized solar cells. Carbon. 2017; 122; 381-388, DOI: 10.1016/j.carbon.2017.06.095.

[32] Huang Yi-June, Lee Chuan-Pei, Pang Hao-Wei, Li Chun-Ting, Fan Miao-Syuan, Vittal R., Ho Kuo-Chuan, Microemulsion-controlled synthesis of $CoSe_2/CoSeO_3$ composite crystals for electrocatalysis in dye-sensitized solar cells. Materials Today Energy. 2017; 6; 189-197, DOI: 10.1016/j.mtener.2017.10.004.

[33] Huang Shoushuang, Ma Dui, Hu ZhangJun, He Qingquan, Zai Jiantao, Chen Dayong, Sun Huai, Chen Zhiwen, Qiao Qiquan, Wu Minghong, Qian Xuefeng, Synergistically enhanced electrochemical performance of Ni_3S_4-PtX (X = Fe, Ni) heteronanorods as heterogeneous catalysts in dye-sensitized solar cells. ACS Applied Materials & Interfaces. 2017; 9; 27607-27617, DOI: 10.1021/acsami.7b05418.

[34] Jin Zhitong, Zhang Meirong, Wang Min, Feng Chuanqi, Wang Zhong-Sheng, Cobalt selenide hollow nanorods array with exceptionally high electrocatalytic activity for high-efficiency quasi-solid-state dye-sensitized solar cells. Journal of Power Sources. 2018; 378; 475-482, DOI: 10.1016/j.jpowsour.2017.12.064.

[35] Geim A. K., Grigorieva I. V., Van der Waals heterostructures. Nature. 2013; 499; 419-425, DOI: 10.1038/nature12385.

[36] Hou Wenjing, Xiao Yaoming, Han Gaoyi, The dye-sensitized solar cells

based on the interconnected ternary cobalt diindium sulfide nanosheet array counter electrode. Materials Research Bulletin. 2018; 107; 204-212, DOI: https://doi.org/10.1016/j.materresbull.2018.07.040.

[37] Chen Haijie, Xie Yian, Cui Houlei, Zhao Wei, Zhu Xiaolong, Wang Yaoming, Lu Xujie, Huang Fuqiang, In situ growth of a $MoSe_2$/Mo counter electrode for high efficiency dye-sensitized solar cells. Chemical Communications. 2014; 50; 4475-4477, DOI: 10.1039/c3cc49600g.

[38] Lemme Max C., Li Lain-Jong, Palacios Tomás, Schwierz Frank, Two-dimensional materials for electronic applications. MRS Bulletin. 2014; 39; 711-718, DOI: 10.1557/mrs.2014.138.

[39] Saadi Fadl H., Carim Azhar I., Velazquez Jesus M., Baricuatro Jack H., McCrory Charles C. L., Soriaga Manuel P., Lewis Nathan S., Operando synthesis of macroporous molybdenum diselenide films for electrocatalysis of the hydrogen-evolution reaction. ACS Catalysis. 2014; 4; 2866-2873, DOI: 10.1021/cs500412u.

[40] Fan Miao-Syuan, Lee Chuan-Pei, Li Chun-Ting, Huang Yi-June, Vittal R., Ho Kuo-Chuan, Nitrogen-doped graphene/molybdenum disulfide composite as the electrocatalytic film for dye-sensitized solar cells. Electrochimica Acta. 2016; 211; 164-172, DOI: 10.1016/j.electacta.2016.06.047.

[41] Ibrahem Mohammed Aziz, Huang Wei-Chih, Lan Tian-wey, Boopathi Karunakara Moorthy, Hsiao Yu-Chen, Chen Chih-Han, Budiawan Widhya, Chen Yang-Yuan, Chang Chia-Seng, Li Lain-Jong, Tsai Chih-Hung, Chu Chih Wei, Controlled mechanical cleavage of bulk niobium diselenide to nanoscaled sheet, rod, and particle structures for Pt-free dye-sensitized solar cells. Journal of Materials Chemistry A. 2014; 2; 11382-11390, DOI: 10.1039/c4ta01881h.

[42] Huang Yi-June, Fan Miao-Syuan, Li Chun-Ting, Lee Chuan-Pei, Chen Tai-Ying, Vittal R., Ho Kuo-Chuan, $MoSe_2$ nanosheet/poly(3,4-ethylenedioxythiophene):poly(styrenesulfonate) composite film as a Pt-free counter electrode for dye-sensitized solar cells. Electrochimica Acta. 2016; 211; 794-803, DOI: 10.1016/j.electacta.2016.06.086.

[43] Mohammadnezhad Mahyar, Liu Mimi, Selopal Gurpreet Singh, Navarro-Pardo Fabiola, Wang Zhming M., Stansfield Barry, Zhao Haiguang, Lai Cheng-Yu, Radu Daniela R., Rosei Federico, Synthesis of highly efficient $Cu_2ZnSnS_xSe_{4-x}$ (CZTSSe) nanosheet electrocatalyst for dye-sensitized solar cells. Electrochimica Acta. 2020 340; 135954-135964, DOI: 10.1016/j.electacta.2020.135954.

[44] Antonelou Aspasia, Syrrokostas George, Sygellou Lamprini, Leftheriotis George, Dracopoulos Vassileios, Yannopoulos Spyros N, Facile, substrate-scale growth of mono and few-layer homogeneous MoS_2 films on Mo foils with enhanced catalytic activity as counter electrodes in DSSCs. Nanotechnology. 2016; 27; 045404-045414, DOI: 10.1088/0957-4484/27/4/045404.

[45] Chiu I. Ting, Li Chun-Ting, Lee Chuan-Pei, Chen Pei-Yu, Tseng Yu-Hao, Vittal R., Ho Kuo-Chuan, Nanoclimbing-wall-like $CoSe_2$/carbon composite film for the counter electrode of a highly efficient dye-sensitized solar cell: A study on the morphology control. Nano Energy. 2016; 22; 594-606, DOI: 10.1016/j.nanoen.2016.02.060.

[46] S Infant Raj, Xu Xiuwen, Yang Wang, Yang Fan, Hou Liqiang, Li Yongfeng, Highly active and reflective MoS_2 counter electrode for enhancement of photovoltaic efficiency of dye sensitized solar cells. Electrochimica Acta. 2016; 212; 614-620, DOI: 10.1016/j.electacta.2016.07.059.

[47] Chiu Jian-Ming, Chen E. Ming, Lee Chuan-Pei, Shown Indrajit, Tunuguntla Venkatesh, Chou Jui-Sheng, Chen Li-Chyong, Chen Kuei-Hsien, Tai Yian, Geogrid-inspired nanostructure to reinforce a $Cu_xZn_ySn_zS$ nanowall electrode for high-stability electrochemical energy conversion devices. Advanced Energy Materials. 2017; 7; 1602210-1602219, DOI: 10.1002/aenm.201602210.

[48] Patil Supriya A., Hussain Sajjad, Shrestha Nabeen K., Mengal Naveed, Jalalah Mohammed, Jung Jongwan, Park Jea-Gun, Choi Hyosung, Kim Hak-Sung, Noh Yong-Young, Facile synthesis of cobaltenickel sulfide thin film as a promising counter electrode for triiodide reduction in dye-sensitized solar cells. Energy. 2020; 202; 117730-117737, DOI: 10.1016/j.energy.2020.117730.

[49] Lee Chi-Ta, Peng Jia-De, Li Chun-Ting, Tsai Yu-Lin, Vittal R., Ho Kuo-Chuan, Ni_3Se_4 hollow architectures as catalytic materials for the counter electrodes of dye-sensitized solar cells. Nano Energy. 2014; 10; 201-211, DOI: 10.1016/j.nanoen.2014.09.017.

[50] Li Chun-Ting, Lee Chuan-Pei, Chiu I. Ting, Vittal R., Huang Yi-June, Chen Tai-Ying, Pang Hao-Wei, Lin Jiann T., Ho Kuo-Chuan, Hierarchical $TiO_{1.1}Se_{0.9}$-wrapped carbon cloth as the TCO-free and Pt-free counter electrode for iodide-based and cobalt-based dye-sensitized solar cells. Journal of Materials Chemistry A. 2017; 5; 14079-14091, DOI: 10.1039/c7ta02474f.

[51] Jiang Xiancai, Li Hongmei, Li Shuolin, Huang Shaowei, Zhu Changli, Hou Linxi, Metal-organic framework-derived Ni–Co alloy@carbon microspheres as high-performance counter electrode catalysts for dye-sensitized solar cells. Chemical Engineering Journal. 2018; 334; 419-431, DOI: 10.1016/j.cej.2017.10.043.

[52] Jiang Yiqing, Qian Xing, Zhu Changli, Liu Hongyu, Hou Linxi, Nickel cobalt sulfide double-shelled hollow nanospheres as superior bifunctional electrocatalysts for photovoltaics and alkaline hydrogen evolution. ACS Applied Materials & Interfaces. 2018; 10; 9379-9389, DOI: 10.1021/acsami.7b18439.

[53] Su Lijun, Xiao Yaoming, Han Gaoyi, Lin Jeng-Yu, One-step hydrothermal synthesis of feather duster-like NiS@MoS_2 with hierarchical array structure for the Pt-free dye-sensitized solar cell. Journal of Nanoparticle Research. 2018; 20; 115-125, DOI: 10.1007/s11051-018-4223-5.

[54] Huang Yi-June, Chen Han-Ting, Ann Shiuan-Bai, Li Chun-Ting, Lin Jiann T., Lee Chuan-Pei, Ho Kuo-Chuan, Hierarchical urchin-like $CoSe_2$/$CoSeO_3$ electrocatalysts for dye-sensitized solar cells: up to 19% PCE under dim light illumination. Journal of Materials Chemistry A. 2019 7; 26089-26097, DOI: 10.1039/C9TA09166A.

[55] Liao Wei, Gao Yuan, Wang Wen, Zuo Xueqin, Yang Qun, Lin Yunxiang, Tang Huaibao, Jin Shaowei, Li Guang, Boosted reactivity of low-cost solar cells over a CuO/Co_3O_4 interfacial structure integrated with graphene oxide. ACS Sustainable Chemistry & Engineering. 2020; 8; 7308-7315, DOI: 10.1021/acssuschemeng.0c00282.

[56] Huang Jie, Qian Xing, Yang Jiahui, Niu Yudi, Xu Chong, Hou Linxi, Construction of Pt-free electrocatalysts based on hierarchical CoS_2/N-doped C@Co-WS_2 yolk-shell nano-polyhedrons for dye-sensitized solar cells. Electrochimica Acta. 2020; 340; 135949-135959, DOI: 10.1016/j.electacta.2020.135949.